



## Short communication

## A transversely isotropic constitutive model of excised guinea pig spinal cord white matter

Beth Galle<sup>a</sup>, Hui Ouyang<sup>b</sup>, Riyi Shi<sup>b,c</sup>, Eric Nauman<sup>a,b,c,\*</sup><sup>a</sup> School of Mechanical Engineering, Purdue University, West Lafayette, IN 47907, USA<sup>b</sup> Department of Basic Medical Sciences, Purdue University, West Lafayette, IN 47907, USA<sup>c</sup> Weldon School of Biomedical Engineering, Purdue University, West Lafayette, IN 47907, USA

## ARTICLE INFO

## Article history:

Accepted 12 June 2010

## Keywords:

Spinal cord injury

SCI

Finite deformation

## ABSTRACT

Narrowing of the spinal canal generates an amalgamation of stresses within the spinal cord parenchyma. The tissue's stress state cannot be quantified experimentally; it must be described using computational methods, such as finite element analysis. The objective of this research was to propose a compressible, transversely isotropic constitutive model, an augmentation of the isotropic Mooney–Rivlin hyperelastic strain energy function, to describe the guinea pig spinal cord white matter. Model parameters were derived from a combination of inverse finite element analysis on transverse compression experiments and least squared error analysis applied to quasi-static longitudinal tensile tests. A comparison of the residual errors between the predicted response and the experimental measurements indicated that the transversely isotropic constitutive law that incorporates an offset stretch reduced the error by a factor of four when compared to other commonly used models.

© 2010 Elsevier Ltd. All rights reserved.

## 1. Introduction

The link between tissue-level mechanical insults to the spinal cord and cellular damage has yet to be established although the problem is clearly multi-axial and multi-scale (Fig. 1) (Panjabi and White, 1988; Blight, 1988). Galle et al. (2007) were the first to relate tissue level stresses to disruption of the axonal membrane in an ex vivo model. Their model considered the plane strain response of a two-dimensional cross-section loaded in transverse compression and correlated physiological damage to strain energy density and various stress components (Galle et al., 2007). That study was followed by one that directly correlated deficits in compound action potentials to tissue level stress fields (Ouyang et al., 2008). This ex vivo model is advantageous because it provides an opportunity to simultaneously measure the applied load, deformation, and functional electrophysiology (Shi and Blight, 1996; Shi, 2004; Shi and Whitebone, 2006). In order to extend this model to multi-axial loading configurations, it is necessary to develop a transversely isotropic constitutive law.

Consequently, the objective of this research was to propose a transversely isotropic, compressible form of the Mooney–Rivlin hyperelastic strain energy function to describe spinal cord tissue mechanics. The parameters for the isotropic form of the

constitutive law were determined using the same inverse FEA process developed by Galle et al. (2007) save that the incompressible constitutive law was replaced with the compressible form. Subsequently, the parameters governing the fiber reinforcement were determined by performing quasi-static uniaxial tensile tests on strips of excised guinea pig spinal cord white matter and performing a least-squares analysis.

## 2. Methods

## 2.1. Specimen acquisition

The procedure used to isolate guinea pig spinal cord white matter has been described previously (Shi and Whitebone, 2006) and was approved by the Purdue University Animal Care and Use Committee. Briefly, adult guinea pigs (bodyweight: ~300 g) were anesthetized and perfused from the heart with cold, oxygenated Krebs solution. The vertebral column was excised immediately following perfusion, the spinal cord was carefully removed, and the pia mater was cut away using micro-scissors. The spinal cord was then separated into two symmetric halves by cutting along the sagittal plane. The gray matter was dissected from the half cords to obtain strips of ventral white matter. Finally, the white matter strips were cut to lengths of approximately 4 cm for testing and stored briefly in oxygenated Krebs solution at room temperature to maintain tissue hydration.

## 2.2. Compression tests

A custom testing system was used for both the transverse compression and axial extension tests. Compression tests were performed on six samples of guinea pig white matter following the procedures described by Galle et al. (2007). Briefly,

\* Correspondence address. 585 Purdue Mall, West Lafayette, IN 47907-2088, USA. Tel.: +1 765 494 8602; fax: +1 765 494 0539.

E-mail address: [enauman@purdue.edu](mailto:enauman@purdue.edu) (E. Nauman).

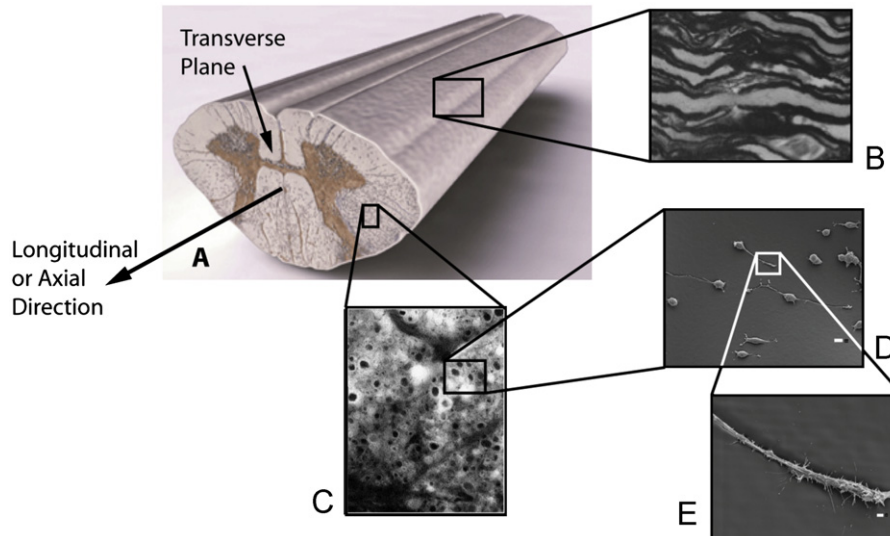


**Fig. 1.** Multi-scale structure of the guinea pig spinal cord (A). The longitudinal direction exhibits a wavy structure that resembles the crimp pattern observed in tendons and ligaments. Individual axons (2–10  $\mu\text{m}$  in diameter), stained black with horseradish peroxidase, can be observed in the transverse section (C). Mechanical loads are ultimately transmitted to the individual cells (D) and may affect the function of membrane-bound proteins in the axons—shown in closeup in (E).

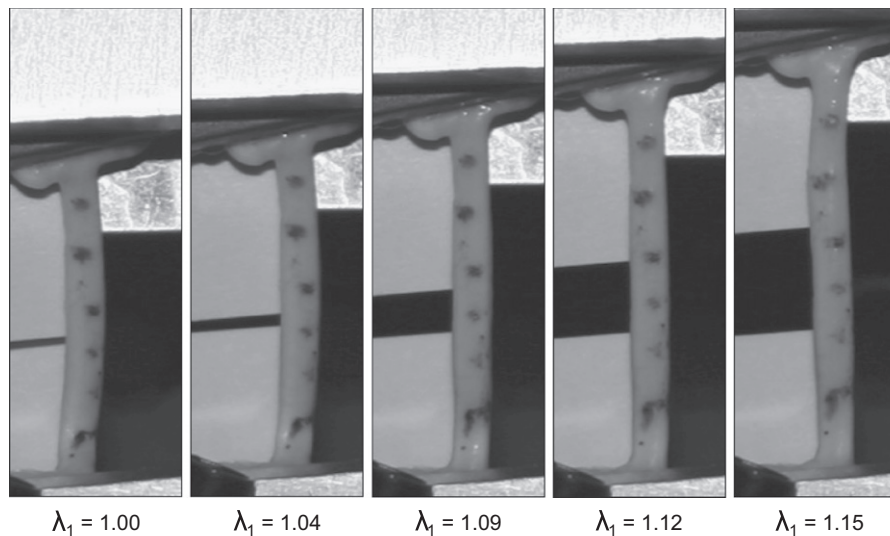


**Fig. 2.** Digital photographs taken during quasi-static uniaxial elongation of a typical guinea pig white matter segment. There is no measurable contraction in the lateral direction.

strips of guinea pig spinal cord white matter ( $n=6$ ) were quasi-statically deformed at a rate of 0.05 mm/s to 90% nominal transverse compression. Force feedback was measured during compression at a rate of 16 Hz.

### 2.3. Axial stretch experiments

Tensile tests, both *in vivo* and *in vitro*, have been described previously within the framework of linear elasticity for a variety of animal models (Hung and Chang, 1981; Hung et al., 1981; Bilston and Thibault, 1996; Ichihara et al., 2001; Ozawa et al., 2001). For the present study quasi-static uniaxial tensile tests ( $n=6$ ) were performed on strips of excised guinea pig spinal cord white matter. Cross-sectional areas of the white matter strips were measured from digital photographs of the tissue ( $2.00 \pm 0.380 \text{ mm}^2$ ). The white matter strip was allowed to hang under its own weight, approximating the *in vivo* length. The white matter strips were uniaxially elongated, without preconditioning, at a quasi-static rate of 0.05 mm/s. Prior to elongation, the tissue was labeled with dots of India ink. The dots were digitally imaged and tracked throughout tissue elongation to quantify  $\lambda_1$ , the principal stretch in the longitudinal direction (Fig. 2) and the applied tensile force was recorded with a Sensotec 1000g load cell (Honeywell, Morristown, NJ) accurate to  $<0.005 \text{ N}$ .

### 2.4. Prediction of the tensile response

In the longitudinal direction, the axons within the white matter extend longitudinally throughout the tissue and the spinal cord parenchyma is devoid of a collagenous, structural extracellular matrix (Shellswell et al., 1979). Consequently, the guinea pig spinal cord white matter was modeled using an isotropic strain energy function,  $W_{\text{iso}}$ , augmented with a reinforcing function,  $W_{\text{fiber}}$ , to represent the axon–myelin bundles,

$$W = W_{\text{iso}} + W_{\text{fiber}}^{\zeta}, \quad (1)$$

where the superscript,  $\zeta$  is used to distinguish between forms of the strain energy function. Material deformations were described by the deformation gradient,  $\mathbf{F}$ , and the invariants  $I_1$ ,  $I_2$ , and  $I_3$  were expressed as functions of  $\mathbf{C} = \mathbf{F}^T \mathbf{F}$ , the right Cauchy–Green deformation tensor,

$$\begin{aligned} I_1 &= \text{tr} \mathbf{C}, \\ I_2 &= \frac{1}{2}[(\text{tr} \mathbf{C})^2 - \text{tr} \mathbf{C}^2], \\ I_3 &= \det \mathbf{C} = J^2, \end{aligned} \quad (2)$$

where  $J$  is the determinant of  $\mathbf{F}$ .

The isotropic, compressible form of the Mooney–Rivlin hyperelastic strain energy function was chosen to model the isotropic matrix of the guinea pig spinal cord white matter (Holzapfel, 2000),

$$W_{\text{iso}}(I_1, I_2) = c_0(J-1)^2 - 2(c_1 + 2c_2)\ln J + c_1(I_1 - 3) + c_2(I_2 - 3), \quad (3)$$

where  $c_0$ ,  $c_1$  and  $c_2$ , are material constants. The second Piola–Kirchhoff stress  $\mathbf{S}_{\text{iso}}$  for the isotropic response was therefore

$$\mathbf{S}_{\text{iso}} = 2 \frac{\partial W_{\text{iso}}}{\partial \mathbf{C}} = 2(c_1 + c_2 I_1) \mathbf{I} - 2c_2 \mathbf{C} + 2[c_0 J(J-1) - (c_1 + 2c_2)] \mathbf{C}^{-1}. \quad (4)$$

The engineering stress, or first Piola–Kirchhoff stress,  $\mathbf{P} = \mathbf{F}\mathbf{S}$ , was used to relate the applied force to the original, un-deformed cross-sectional area.

While most soft tissues are nearly incompressible in their natural environment, the water content is typically restricted by a surrounding membrane, the incompressibility assumption does not hold when the surrounding membrane is disrupted and water is allowed to escape from the tissue as is the case for most ex vivo experiments. Without the reinforcement of the pia matter, the white matter specimens demonstrated no measurable contraction in the lateral directions when a stretch was applied in the 1-direction (Fig. 2).

For an axial stretch, the tissue deformation can be described in terms of the principal stretches

$$\mathbf{F} = \begin{bmatrix} \lambda_1 & 0 & 0 \\ 0 & \lambda_2 & 0 \\ 0 & 0 & \lambda_3 \end{bmatrix}. \quad (5)$$

For the purposes of this study, the reinforcing functions were assumed to depend on the pseudo-invariant  $I_4 = \mathbf{a}_0 \cdot \mathbf{C}\mathbf{a}_0$  only, where the unit vector  $\mathbf{a}_0$  specified the fiber direction within the material. The fiber, or axon, direction is given by the unit vector  $\mathbf{a}_0 = [1 \ 0 \ 0]$ . Four forms of the fiber reinforcing

function (Weiss et al., 1996; Holzapfel, 2000; Weiss and Gardiner, 2001; Merodio and Ogden, 2003, 2005) were chosen for comparison (Table 1).

### 2.5. Parameter estimation

We have previously presented the force–deformation response of the guinea pig spinal cord white matter to quasi-static transverse compression (Galle et al., 2007). In our earlier work, we compared the force–deflection curves from the transverse compression experiments to a plane strain computational model of the white matter. Inverse FEA was then used to determine the material parameters corresponding to an incompressible Mooney–Rivlin constitutive law. For this study, we allowed for compressibility of the parenchyma and repeated the process described previously (Galle et al., 2007). The strain energy function was implemented as a plane strain, parametric FEM (Software: COMSOL 3.2 with MATLAB, Comsol, Burlington, MA). The material parameters  $c_0$ ,  $c_1$ , and  $c_2$  were found by minimizing the error between the predicted force–deflection curve and the measured relationship (Galle et al., 2007).

A similar process was used to obtain the coefficients for each of the reinforcing functions from the longitudinal force–deflection response. For longitudinal extension, the procedure was considerably simpler because the deformation was assumed to be homogeneous. Consequently, the analytical relationships between  $P_{11}$  and the measured stretch (Table 1) were curve fit to the experimental data using a least squared error minimization procedure.

## 3. Results

The material parameters,  $c_0$ ,  $c_1$ , and  $c_2$ , were determined for each sample and the average values were used for the subsequent

**Table 1**  
Strain energy functions and stress–stretch response for five reinforcing functions.

Reinforcing function	Strain energy function	Stress–stretch response
Isotropic model		$P_{11}^{\text{iso}} = \frac{F(\lambda_1)}{A_0} = 2c_0(\lambda_1 - 1) + 2(c_1 + 2c_2) \left( \lambda_1 - \frac{1}{\lambda_1} \right)$
Standard reinforcing function	$W_{\text{fiber}}^1(I_4) = \frac{\alpha}{2}(I_4 - 1)^2$	$P_{11}^1 = 2c_0(\lambda_1 - 1) + 2(c_1 + 2c_2) \left( \lambda_1 - \frac{1}{\lambda_1} \right) + 2\alpha(\lambda_1^3 - \lambda_1)$
Ligament exponential	$W_{\text{fiber}}^2(I_4) = \beta[\exp(I_4 - 1) - I_4]$	$P_{11}^2 = 2c_0(\lambda_1 - 1) + 2(c_1 + 2c_2) \left( \lambda_1 - \frac{1}{\lambda_1} \right) + 2\beta\lambda_1 [\exp(\lambda_1^2 - 1) - 1]$
Cardiac exponential	$W_{\text{fiber}}^3(I_4) = \delta [\exp(I_4 - 1)^2 - 1]$	$P_{11}^3 = 2c_0(\lambda_1 - 1) + 2(c_1 + 2c_2) \left( \lambda_1 - \frac{1}{\lambda_1} \right) + 4\delta(\lambda_1^3 - \lambda_1) [\exp(\lambda_1^2 - 1)^2]$
Modified exponential	$W_{\text{fiber}}^4(I_4) = \gamma [\exp(I_4 - 1)^2 - (I_4 - 1)^2 - 1]$	$P_{11}^4 = 2c_0(\lambda_1 - 1) + 2(c_1 + 2c_2) \left( \lambda_1 - \frac{1}{\lambda_1} \right) + 4\gamma(\lambda_1^3 - \lambda_1) \left\{ \exp(\lambda_1^2 - 1)^2 \right\}$
Offset stretch	$W_{\text{fiber}}^5(I_4) = \frac{\eta}{2} [I_4 - f_{\text{offset}}(\lambda_1)]^2$ ,  $f_{\text{offset}}(\lambda_1) = \begin{cases} \lambda_1^2, & \lambda_1 < \lambda_{\text{offset}} \\ \lambda_{\text{offset}}^2, & \lambda_1 \geq \lambda_{\text{offset}} \end{cases}$	$P_{11}^5 = \begin{cases} 2c_0(\lambda_1 - 1) + 2(c_1 + 2c_2) \left( \lambda_1 - \frac{1}{\lambda_1} \right), & \lambda_1 < \lambda_{\text{offset}} \\ 2c_0(\lambda_1 - 1) + 2(c_1 + 2c_2) \left( \lambda_1 - \frac{1}{\lambda_1} \right) + \eta\lambda_1(\lambda_1^2 - \lambda_{\text{offset}}^2), & \lambda_1 \geq \lambda_{\text{offset}} \end{cases}$

**Table 2**  
Parameter estimation and residuals for each model type.

Model type	Parameter	Mean ± Std dev.	Average residual (kPa)
Isotropic model	$c_0$ (kPa)	0.412 ± 0.339	0.651
	$c_1$ (kPa)	0.876 ± 0.625	
	$c_2$ (kPa)	0.614 ± 0.234	
Standard reinforcing function	$\alpha$ (kPa)	71.7 ± 70.9	0.297
Ligament exponential	$\beta$ (kPa)	67.3 ± 70.5	0.276
Cardiac exponential	$\delta$ (kPa)	34.7 ± 36.1	0.270
Modified exponential	$\gamma$ (kPa)	5,314 ± 10,647	0.080
Offset stretch	$\lambda_{\text{offset}}$ (No units)	1.083 ± 0.063	0.041
	$\eta$ (kPa)	201 ± 146	

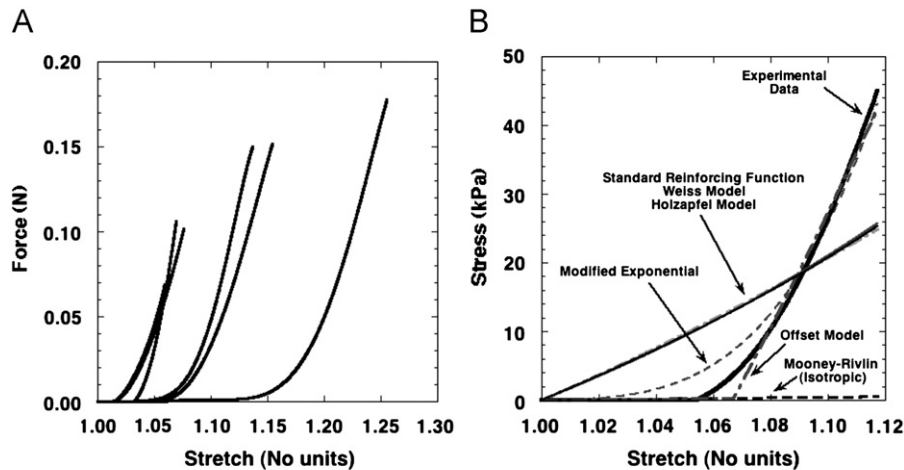


**Fig. 3.** Experimental force–deflection relationship for six ventral white matter specimens (A) and an example stress–stretch response for a single specimen (B). The results of the curve fits for the isotropic Mooney–Rivlin model and the five different reinforcing functions examined herein are superposed (B). The best fit was obtained from the offset stretch model.

analysis of the axial loading experiments (Table 2). The worst fit to the experimental data was obtained from the isotropic model while the best fit was obtained using the offset model (Fig. 3).

#### 4. Discussion

Slow compression spinal cord injuries occur when the spinal canal cross-section is narrowed, the consequence of oncologic, infective, or degenerative lesion growth. The narrowed canal gradually compresses the spinal cord parenchyma until neurological deficit results. Cellular injury is localized within the white matter, as blood flow to and oxygen levels within the gray matter are typically maintained during slow compression. Hallmarks of white matter cellular injury include vacuolization, loss of myelin, and axonal swelling (Kraus, 1996). Further study of the process by which multi-axial mechanical insults create physiological defects requires the development of a transversely isotropic constitutive model.

Herein, we chose to adapt the Mooney–Rivlin hyperelastic constitutive model to describe guinea pig spinal cord white matter mechanics and to utilize an inverse FEA approach to determine the material parameters. Of all the models considered here, the offset stretch model provided the smallest residual error and the least sensitive set of parameters. In particular it should be noted that this model formulation has a physiological basis in the crimp-like structure exhibited at the axonal level. This is the first attempt to model the transverse isotropy of the spinal cord white matter and will provide a basis for evaluating the mechanics of decompression surgery as well as a foundation for studying the viscoelastic and high strain rate response of human spinal cords. It should be noted, however, that spinal cord injuries are often caused by complex, multi-axial deformations for which more comprehensive constitutive laws may be appropriate (Holzapfel et al., 2000). In addition, it is likely that some of the variation observed in the force–stretch data (Fig. 3) is due to the statistical distributions in axon–myelin bundle stiffness (Billiar and Sacks, 2000) and initial crimp angle. Additional studies coupling computational models with multi-axial loading experiments are required to fully elucidate the structure–function properties of the spinal cord.

#### Conflict of interest statement

The authors have no conflict of interest with regard to the publication of this study.

#### Acknowledgements

The authors acknowledge support from the Purdue Research Foundation, Discovery Park at Purdue University, and the State of Indiana, as well as the technical contributions of Gary Leung and artistic contributions of Michel Schweinsberg.

#### References

- Billiar, K.L., Sacks, M.S., 2000. Biaxial mechanical properties of the natural and glutaraldehyde treated aortic valve cusp—Part II: a structural constitutive model. *J. Biomech. Eng.* 122, 327–335.
- Bilston, L.E., Thibault, L.E., 1996. The mechanical properties of the human cervical spinal cord in vitro. *Ann. Biomed. Eng.* 24 (1), 67–74.
- Blight, A., 1988. Mechanical factors in experimental spinal cord injury. *J. Am. Paraplegia Soc.* 11 (2), 26–34.
- Galle, B., Ouyang, H., et al., 2007. Correlations between tissue-level stresses and strains and cellular damage within the guinea pig spinal cord white matter. *J. Biomech.* 40 (13), 3029–3033.
- Holzapfel, G.A., 2000. *Nonlinear Solid Mechanics: A Continuum Approach for Engineering*. Wiley, Chichester, New York.
- Holzapfel, G.A., Gasser, T.C., et al., 2000. A new constitutive framework for arterial wall mechanics and a comparative study of material models. *J. Elasticity* 61, 1–48.
- Hung, T.K., Chang, G.L., 1981. Biomechanical and neurological response of the spinal cord of a puppy to uniaxial tension. *J. Biomech. Eng.* 103 (1), 43–47.
- Hung, T.K., Chang, G.L., et al., 1981. Stress–strain relationship and neurological sequelae of uniaxial elongation of the spinal cord of cats. *Surg. Neurol.* 15 (6), 471–476.
- Ichihara, K., Taguchi, T., et al., 2001. Gray matter of the bovine cervical spinal cord is mechanically more rigid and fragile than the white matter. *J. Neurotrauma* 18 (3), 361–367.
- Kraus, K.H., 1996. The pathophysiology of spinal cord injury and its clinical implications. *Semin. Vet. Med. Surg. (Small Anim.)* 11 (4), 201–207.
- Merodio, J., Ogden, R.W., 2003. Instabilities and loss of ellipticity in fiber-reinforced compressible non-linearly elastic solids under plane deformation. *Int. J. Solids Struct.* 40 (18), 4707–4727.
- Merodio, J., Ogden, R.W., 2005. Mechanical response of fiber-reinforced incompressible non-linearly elastic solids. *Int. J. Non-Linear Mech.* 40 (2–3), 213–227.
- Ouyang, H., Galle, B., et al., 2008. Biomechanics of spinal cord injury: a multimodal investigation using ex vivo guinea pig spinal cord white matter. *J. Neurotrauma* 25 (1), 19–29.

- Ozawa, H., Matsumoto, T., et al., 2001. Comparison of spinal cord gray matter and white matter softness: measurement by pipette aspiration method. *J. Neurosurg.* 95 (2 Suppl), 221–224.
- Panjabi, M., White 3rd, A., 1988. Biomechanics of nonacute cervical spinal cord trauma. *Spine* 13 (7), 838–842.
- Shellswell, G.B., Restall, D.J., et al., 1979. Identification and differential distribution of collagen types in the central and peripheral nervous systems. *FEBS Lett.* 106 (2), 305–308.
- Shi, R., 2004. The dynamics of axolemmal disruption in guinea pig spinal cord following compression. *J. Neurocytol.* 33 (2), 203–211.
- Shi, R., Blight, A.R., 1996. Compression injury of mammalian spinal cord in vitro and the dynamics of action potential conduction failure. *J. Neurophysiol.* 76 (3), 1572–1580.
- Shi, R., Whitebone, J., 2006. Conduction deficits and membrane disruption of spinal cord axons as a function of magnitude and rate of strain. *J. Neurophysiol.* 95 (6), 3384–3390.
- Weiss, J.A., Gardiner, J.C., 2001. Computational modeling of ligament mechanics. *Crit. Rev. Biomed. Eng.* 29 (3), 303–371.
- Weiss, J.A., Maker, B.N., et al., 1996. Finite element implementation of incompressible, transversely isotropic hyperelasticity. *Comput. Methods Appl. Mech. Eng.* 135, 107–128.